Steel and Composite Structures, *Vol. 14, No. 6 (2013) 571-586*
DOI: http://dx.doi.org/10.12989/scs.2013.14.6.571

Non-linear stability analysis of a hybrid barrel vault roof

Jianguo Cai*[1], Ya Zhou[1a], Yixiang Xu[2] and Jian Feng[1]

[1]Key Laboratory of C & PC Structures of Ministry of Education, National Prestress Engineering Research Center, Southeast University, Si Pai Lou 2#, Nanjing 210096, China
[2]Department of Civil Engineering, Strathclyde University, 16 Richmond Street, Glasgow G1 1XQ, Scotland, United Kingdom

(Received August 17, 2011, Revised April 25, 2013, Accepted May 23, 2013)

Abstract. This paper focuses on the buckling capacity of a hybrid grid shell. The eigenvalue buckling, geometrical non-linear elastic buckling and elasto-plastic buckling analyses of the hybrid structure were carried out. Then the influences of the shape and scale of imperfections on the elasto-plastic buckling loads were discussed. Also, the effects of different structural parameters, such as the rise-to-span ratio, beam section, area and pre-stress of cables and boundary conditions, on the failure load were investigated. Based on the comparison between elastic and elasto-plastic buckling loads, the effect of material non-linearity on the stability of the hybrid barrel vault is found significant. Furthermore, the stability of a hybrid barrel vault is sensitive to the anti-symmetrical distribution of loads. It is also shown that the structures are highly imperfection sensitive which can greatly reduce their failure loads. The results also show that the support conditions pose significant effect on the elasto-plastic buckling load of a perfect hybrid structure.

Keywords: stability; non-linear; hybrid structure; cable; elasto-plastic; failure load

1. Introduction

A hybrid barrel vault carries its loads mainly by compression. Therefore analysis of the static stability of a hybrid barrel vault is essential to the design of the structures. Just like single-layer reticulated shells, the necessity of stability check is enhanced by the fact that the hybrid barrel vault can be regarded as a mixture of slab structure and continuum shell thus showing the stability failure of both types and even combinatorial modes (Bulenda and Knippers 2001).

The non-linear buckling analysis procedures for single-layer reticulated shells based upon non-linear finite element (FE) analysis have been developed to trace the equilibrium path by many researchers (Forman and Hutchinson 1970, Meek and Tan 1984, Gioncu 1995, Borri and Spinelli 1998, Nie 2003, Gosowski 2003, Gioncu 2003). The structural behaviour of the shell structures during the whole loading process can be revealed by the load–deflection curves, by which the buckling load can be predicted. The elastic stability of the hybrid barrel vault has been well studied by Bulenda and Knippers (2001). However, the analysis of elasto-plastic stability is much more complicated than the elastic analysis, since the elasto-plastic analysis involves both geometrical and material non-linearities. The elasto-plastic stability of the single-layer reticulated shells has

*Corresponding author, Ph.D., E-mail: j.cai@seu.edu.cn

http://www.techno-press.org/?journal=scs&subpage=8 ISSN: 1229-9367 (Print), 1598-6233 (Online)

attracted more and more attentions of researchers recently (Nee and Halder 1988, Luo 1991, Suzuki *et al*. 1992, Kato *et al*. 2000, Fan *et al*. 2010a, b). With the fast development of computer technology and the availability of advanced FE softwares, it is now possible to conduct a comprehensive study on the stability of the barrel vault through geometrical and material non-linear analyses.

With the development of modern buildings, the appeal of glass roofs grows with their translucence. Barrel vaults with quadrangular mesh are one of the best candidates for transparent glass roofs. However, El-Sheikh (2001a, b) pointed out that a vault with quadrangular mesh lack integration between its segments, which is essential for a reliable structural action especially when the vault is acting as a beam or suffers local damage. Moreover, the vaults become most dependent on the joint rigidity. These serious shortfalls in structural performance outweigh the apparent benefits in reducing the number and length of members used and might limit these vaults to applications with short spans and light loadings. Cables are light and can provide well-defined transmission of forces. They can also been constructed to a structural system with a rational layout of members so as to make the best use of individual material properties (Hosozawa *et al*. 1999). Therefore, they are used in many hybrid string structures, such as beam string structures (Saitoh and Okada 1999, Xue and Liu 2008), and suspend-dome structures (Kang *et al*. 2003, Kitipornchai *et al*. 2005). To achieve high performance of the barrel vault with quadrangular mesh, a hybrid barrel vault roof is proposed (Schlaich and Schober 1996), as shown in Fig. 1.

This paper shows how to perform a geometrical and material non-linear finite element analysis by using ANSYS to investigate the stability of the hybrid barrel vault. The imperfection sensitivity including the pattern and scale of imperfections will be investigated. Additionally, the effect of factors such as the geometrical and structural parameters and the anti-symmetrical distribution of loads will also be taken into consideration in this paper.

2. Stability behavior of barrel vault roofs

The design example used in this study is shown in Fig. 2. The span and rise of the barrel vault structure are 20 m and 5.2 m, respectively (making the rise-span ratio 0.26). All nodes at the perimeter are fixed to the supports. The principal members of the single-layer steel trusses are made of steel with a Young's modulus of 206 GPa, and the cross-section is 120 mm $\times$ 60 mm $\times$ 4 mm (height $\times$ width $\times$ thickness). The diameter of cables is 10 mm and the Young's modulus is 180GPa. The initial stress of cables is 100 MPa. The symmetrical load case $g + s$ (dead load + snow load) has been taken into account in all computations. The dead load g consists of a self-weight of 0.5 kN/m^2 including all beams and cables. The snow load is applied to the top surface of the structure in the vertical direction with a magnitude of 0.5 kN/m^2.

The Finite Element Analysis software ANSYS is employed in all structural analyses that have taken into account the geometrical non-linearity. Tension-only element LINK10 is used to model cables and BEAM 189 is chosen to simulate steel beams.

2.1 Linear eigenvalue buckling analysis

The eigenvalue buckling analysis predicts the theoretical buckling capacity (the bifurcation load) of an ideal linear elastic structure. Although imperfections and material non-linearities often prevent most practical structures from achieving the theoretical elastic buckling capacity, the

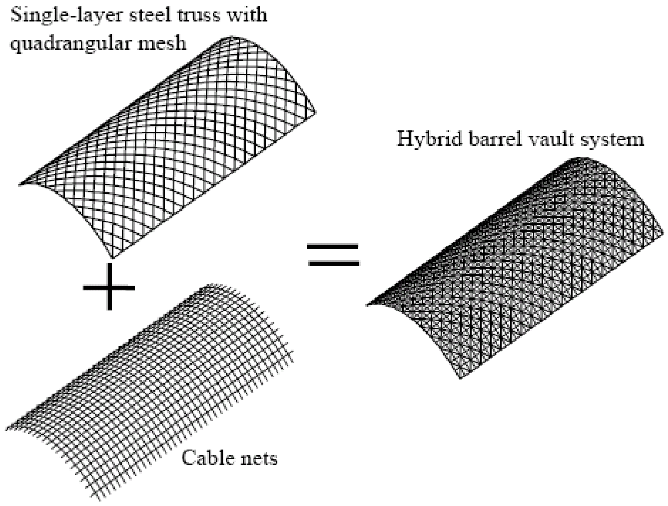

Fig. 1 The hybrid barrel vault system

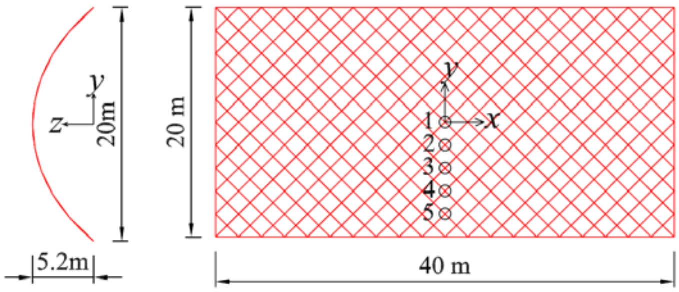

Fig. 2 The design model of the hybrid barrel vault with typical nodes and element numbers

eigenvalue buckling analysis is still a very useful tool to estimate the critical load and buckling modes for single-layer reticulated shells. The buckling results are summarized in Table 1. Some buckling modes of the structure under symmetrical loads are shown in Fig. 3. It is clear from the figure that the first buckling mode is a global one, whereas the sixteenth is found to be the first local mode.

Table 1 Buckling load factors of hybrid barrel vaults

No. of mode	Buckling load factor	No. of mode	Buckling load factor
1	4.415	6	12.426
2	7.301	7	13.534
3	7.894	8	17.068
4	11.315	9	17.315
5	11.427	10	17.923

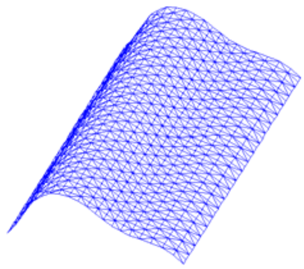

(a) The first mode

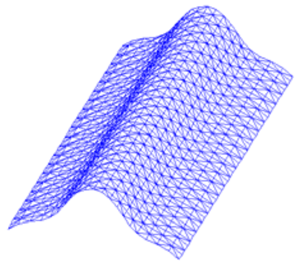

(b) The second mode

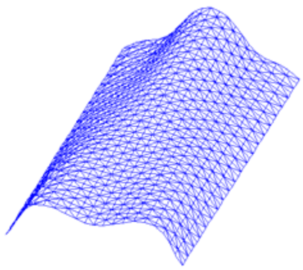

(c) The third mode

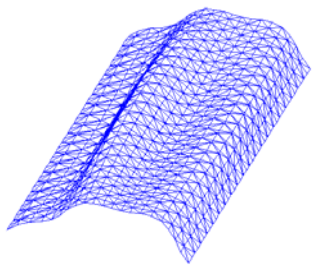

(d) The sixth mode

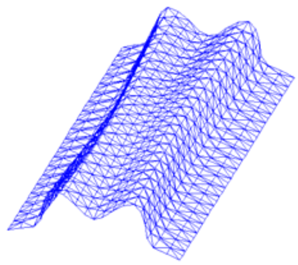

(e) The tenth mode

Fig. 3 Buckling modes of the hybrid barrel vault

2.2 Geometrical non-linear buckling analysis

This section focuses on the buckling analysis of the hybrid barrel vault and considers geometrical non-linearity. Fig. 2 shows the typical nodes of the hybrid structure. The relationship between the displacement at typical nodes and the load factor is shown in Fig. 4. The initial non-zero vertical nodal displacement (with the load factor being zero) is introduced by the cable pre-stress of 100 MPa. All the sub-figures of Fig. 3 are plotted in the same scale for comparison. The vertical displacement of node 1 is notable, also reinforced by Fig. 5 which shows the deformed shape of the hybrid barrel vault in buckling. It can be seen from this figure that the buckling mode is the combination of local and global instability. The critical buckling load factor (7.05) can be obtained from any sub-figure of Fig. 4.

2.3 Elasto-plastic stability analysis

The elasto-plastic stability analysis of the hybrid barrel vault is carried out using ANSYS. The Newton-Raphson method is used to obtain the total load-displacement equilibrium path. The load factor-displacement curves for typical nodes are illustrated in Fig. 6. It is clear from the figure that the buckling capacity of the hybrid barrel vault is rapidly reduced when material non-linearity is considered. Elasto-plastic steel material is adopted, whose yield stress is 345 MPa. The critical buckling load factor obtained from Fig. 6 is 5.64. It can also be found that the maximum displacement of node 1 decreases from 0.49 m found by geometrical non-linear analysis to 0.15 m by elasto-plastic analysis.

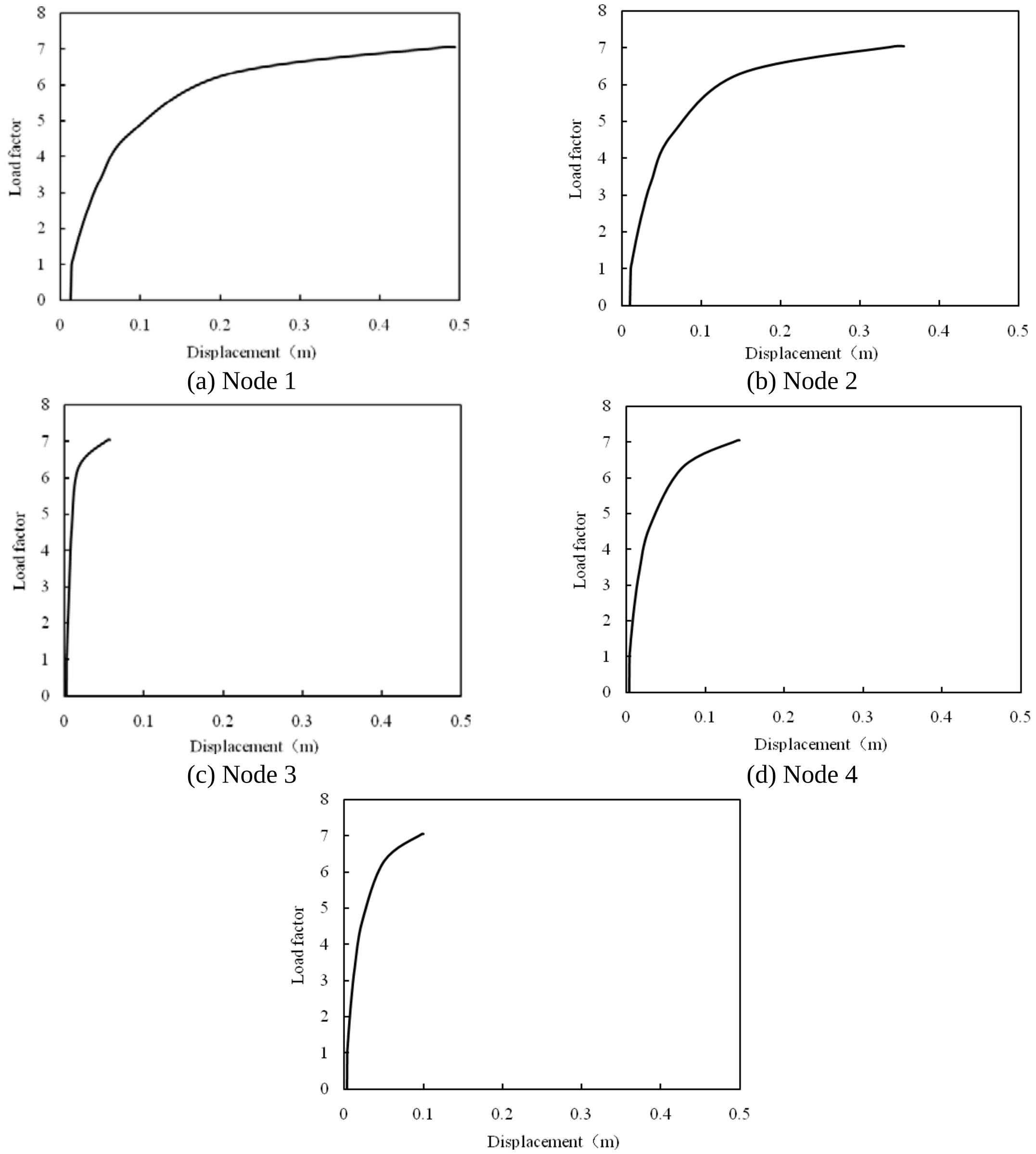

(a) Node 1

(b) Node 2

(c) Node 3

(d) Node 4

(e) Node 5

Fig. 4 Load factor vs. displacement for geometrical non-linear buckling analysis

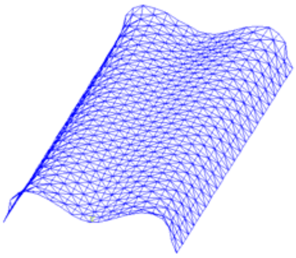

(a) symmetrical loads

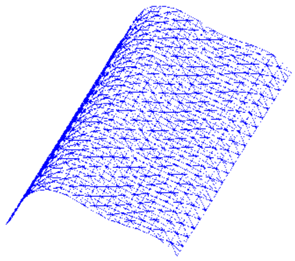

(b) anti-symmetrical loads

Fig. 5 Deformed shape of the hybrid barrel vault in geometrical non-linear buckling analysis

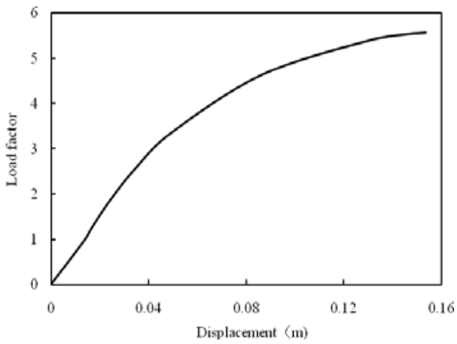

(a) Node 1

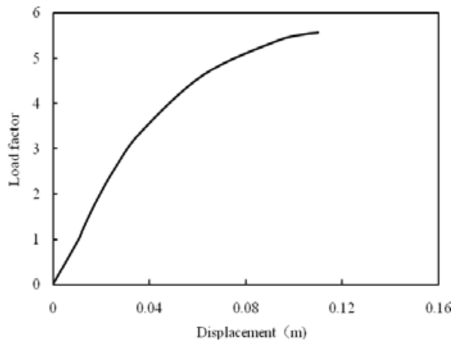

(b) Node 2

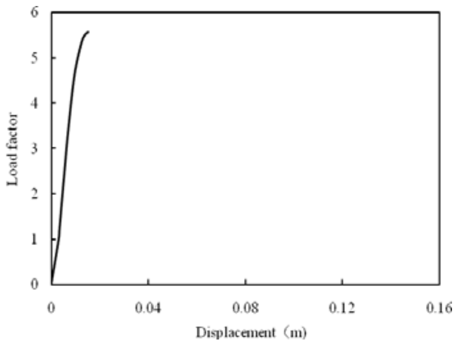

(c) Node 3

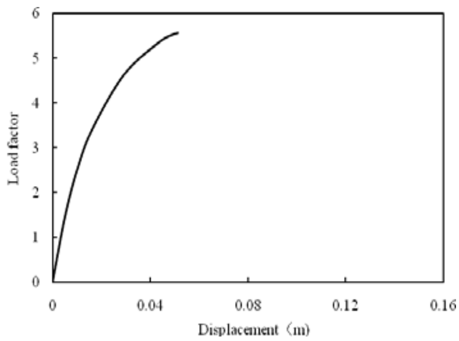

(d) Node 4

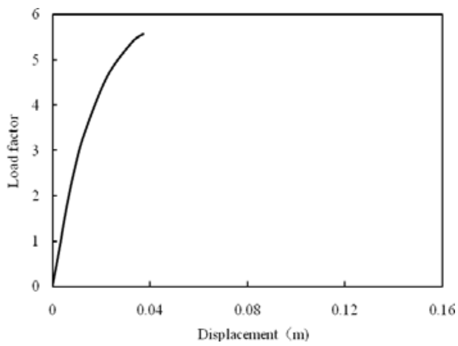

(e) Node 5

Fig. 6 The load factor-displacement curves for elasto-plastic stability analysis

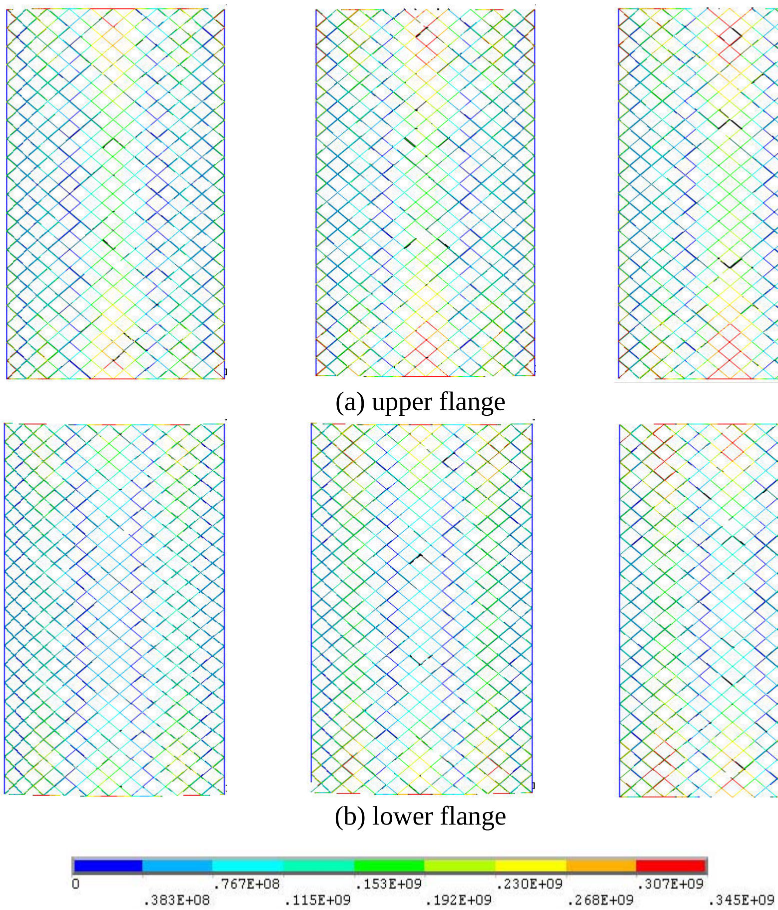

Fig. 7 The development process of the plastic zone (Pa)

The process of developing plastic zone is shown in Fig. 7. The steel box member is in bending and axial compression. Therefore, the plastic zone highlighted in red color is mainly developed on the upper and lower flange of the box member. It is clear from the figure that the plastic zone is firstly formed on both ends of the structure, and then gradually developed towards the middle of the structure until the structure reaches failure.

2.4 Influence of anti-symmetrical loads

Anti-symmetrical load case is an important factor that affects the elasto-plastic buckling capacity of hybrid barrel vaults. One type of anti-symmetrical load is the half-span load which can be resulted during construction or from snow. The anti-symmetrical load case $g + s/2$ (g – dead load and s – snow load, uniformly distributed over half of the span) is considered in this study.

Fig. 8 shows the load factor-displacement curves for typical nodes under the anti-symmetrical load case. The critical buckling load factor obtained from Fig. 8 is 3.72, which is 34% lower than the critical buckling load factor (5.64) for symmetrical loads. It can be concluded that the anti-

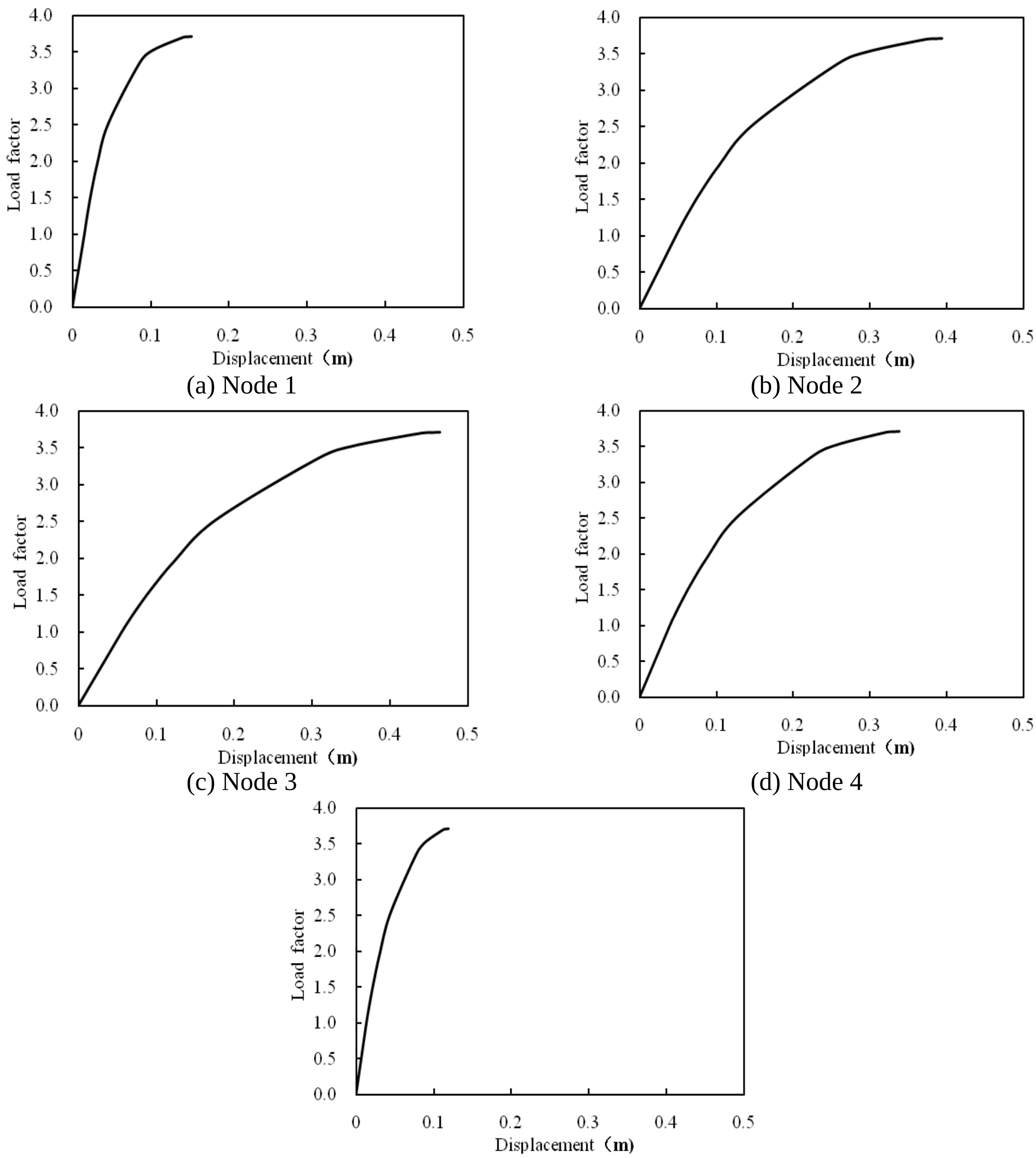

(a) Node 1 (b) Node 2

(c) Node 3 (d) Node 4

(e) Node 5

Fig. 8 The load factor-displacement curves for the anti-symmetrical load case

symmetrical distribution of load poses very large effect on the buckling load from the geometrical and material non-linear analysis.

3. Geometric imperfections

Shell structures are very sensitive to geometric imperfections which are inevitable during fabrication. There are several types of imperfections in all practical structures: imperfections of the system (e.g., non-rigid joints); structural imperfections (tolerances of the cross-section area, non-homogeneous materials, etc.), loading imperfections, and geometrical imperfections (Bulenda and Knippers 2001). According to the European standard (2004) and Chinese code (JGJ61 2003), the geometrical imperfection should be taken into account in the non-linear analysis in order to model the structure in a realistic way.

Several methods are available to analyze geometrical imperfections, i.e., the random imperfection mode method (Yamada 2001), the consistent imperfection mode method (Chen and Shen 1993). In the former method, samples distributed with randomly generated imperfections are studied. The sample with the smallest buckling capacity is identified, and the corresponding buckling capacity is treated as the approximated critical capacity of the system. In the later method, the imperfection distribution is assumed to be consistent with deflected shapes, such as eigenvalue buckling modes. The consistent imperfection mode method is used in this paper. Then the shape and the scale of the geometric imperfection will be discussed.

3.1 Shape of the imperfection

Normally, the first eigenvalue buckling mode is chosen as the imperfection shape. This is also called the fundamental mode imperfection method (JGJ61 2003) or the eigenmode imperfection method (European standard 2004). Generally, the buckling capacity that is calculated by the fundamental mode imperfection method is lower than those given by higher eigenvalue buckling modes, e.g., single-layer reticulated shells. However, for a pre-stressed space structure, Zhang *et al*. (2006) stated that the buckling capacity based on other eigenvalue buckling modes may be the lowest. On the other hand, Bulenda and Knippers (2001) suggested using the final buckling shape as a geometrical imperfection.

Therefore, shapes of imperfections for the hybrid barrel vault are set up as follows: (1) The first several eigenvalue buckling modes; (2) the displacement shape of the loaded structure obtained from a geometrical non-linear elastic buckling analysis. Both imperfections are easy to compute and therefore can be often used by engineers.

3.2 Scale of the imperfection

The scaling of the imperfection is as important as its shape. Generally, the span of the structure is taken as a reference scale for the imperfection size (European standard 2004). According to the specifications of the Chinese lattice dome (JGJ61 2003), the maximum geometric imperfection that is caused by construction should be restricted within span / 300. As expected, the buckling capacity of the structure decreases when the maximum nodal displacement due to the geometric imperfection increases. However, for a hybrid structure, the buckling capacity with the maximum imperfection of span / 300 may not be the lowest (Zhang *et al*. 2006). Therefore, we need to vary the imperfection scale in order to assess the imperfection sensitivity of the structure.

3.3 Results of different imperfection shapes

Figs. 3 and 5 show the eigenmodes of the hybrid structure obtained from eigenvalue analyses, and the deformed shapes found by geometrical non-linear analyses with loading cases $g+s$ (Load 1) and $g+s/2$ (Load 2), respectively. These shapes are used to import imperfections.

Figs. 9 and 10 show the load-displacement curves for different hybrid barrel vaults, including the perfect structure as well as the structures imposed on six different imperfect shapes. The load is plotted against a nodal displacement in the area of maximum deformation. The maximum imperfections of all shapes have been scaled to span / 300. For the model in this study, the span is 20 m, and thus the maximum geometric imperfection is 66.7 mm. The perfect system exhibits a failure load, which is 5.64 and 3.72 times the design load for symmetrical load and anti-symmetrical load cases, respectively.

The load-displacement curves for the structure with imperfections based on eigenmodes or deformed shapes of the loading cases show the similar trend with the perfect structure. It is clear from the figure that the failure load of the hybrid structure under the symmetrical load $g+s$ is rapidly reduced in the presence of geometric imperfections. The lowest buckling load is predicted with the first eigenvalue buckling mode. In this case the failure load is 4.2 times the design load, a 25% reduction in the failure load. Therefore, our comparison shows large influence of different

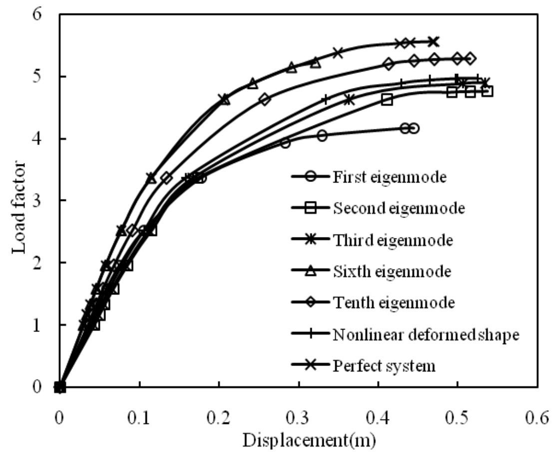

Fig. 9 Load-displacement curves for imperfect structures, loading case *g+s*

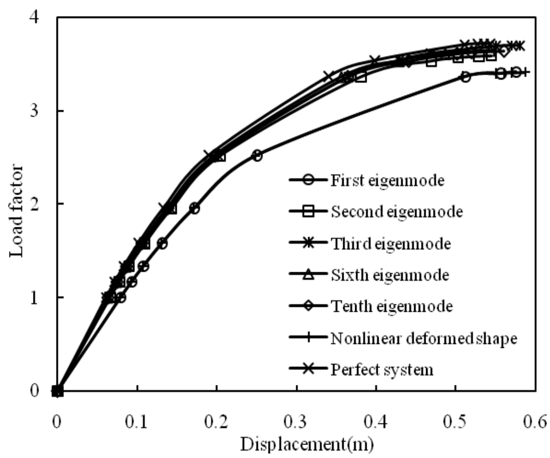

Fig. 10 Load-displacement curves for imperfect structures, loading case *g+s/2*

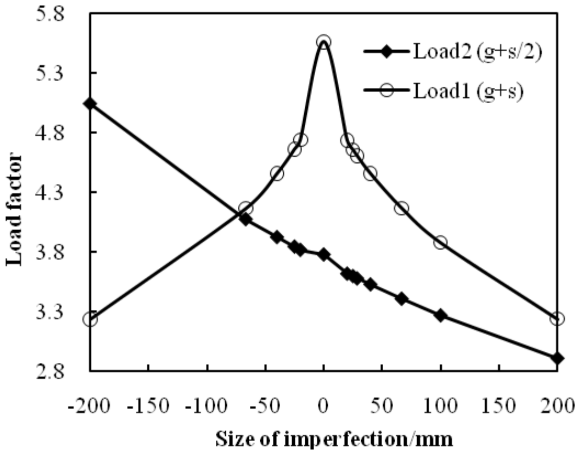

Fig. 11 Imperfection sensitivity

shapes of imperfections on the failure load under the symmetrical load. The first eigenvalue buckling mode shows the largest reduction of the failure load compared to imperfection based on other buckling shapes.

All of the imperfections reduce the failure load slightly under the anti-symmetrical load case $g + s/2$. The lowest failure load factor is 3.4, which is 10.5% lower than that of a perfect structure. The critical imperfect shape is the deformed shape obtained from a geometrical non-linear elastic buckling computation. It should be noted that the failure load in this case is almost identical to that of a structure with an imperfection based on the first eigenmode. Furthermore, the comparison between the curves for the loading case $g+s$ and those for $g+s/2$ shows the higher failure loads in the former case.

In comparison of the complexity of implementation and the previous results, the first eigenmode imperfection can be straightforwardly obtained by a linear-elastic eigenvalue buckling analysis and is shown the most critical imperfection shape. This imperfection shape is thus employed in all the following analyses.

It can also be found from Fig. 11 that the hybrid structure shows relatively little sensitivity to imperfections when the structure is under the anti-symmetrical load $g+s/2$. It is very interesting to note that the failure load reduces when the imperfection scale increases regardless of its sign. The failure load with negative imperfection scale is higher than that of the perfect structure. Therefore, it is important to know in which direction the imperfection is imposed.

4. Numerical modelling

4.1 The influence of the rise-to-span ratio

The elasto-plastic analyses have been carried out based on sample structures with different rises (keeping the span constant). The failure loads are shown in Fig. 12. The rise-to-span ratios correspond to 0.13, 0.2, 0.26, 0.38 and 0.47, respectively. For the structure under the symmetrical load $g+s$, if the rise-span ratio is smaller than 0.26, an increase in rise-to-span ratio will result in

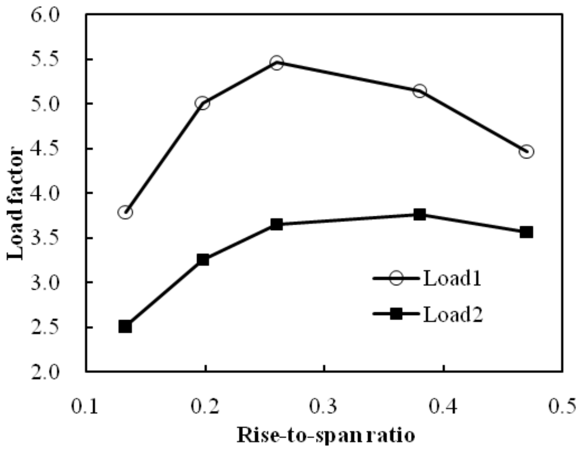

Fig. 12 Failure loads with different rise-to-span ratios

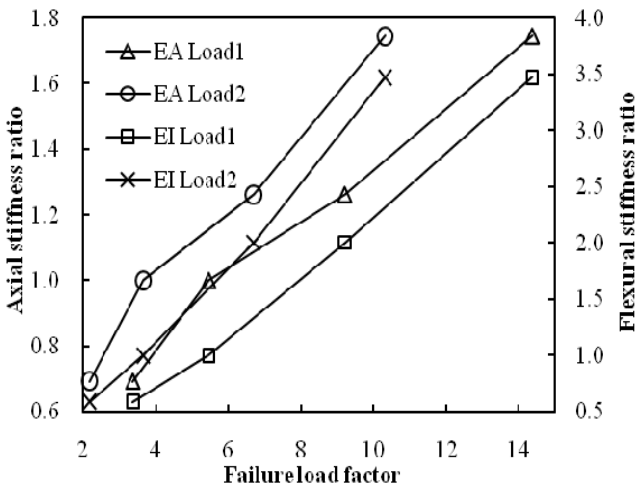

Fig. 13 Failure loads with different cross-sections of steel beams

an increase in the failure load. If the rise-to-span ratio greater than 0.26, a higher rise-to-span ratio gives a lower failure load. A similar trend can be found when the structure is under the anti-symmetrical load $g+s/2$. Therefore, the structure may have a highest failure load at a specific rise-to-span ratio. It can be concluded that there may exits an optimal value of rise-to-span ratio for a specific hybrid barrel vault roof.

4.2 The influence of the cross-sections of steel beams

When the geometry of the structure is identified, the cross-section of steel beams is an important factor that affects the buckling capacity of the hybrid barrel vault. Fig. 13 shows the variations of the axial stiffness and the flexural stiffness of steel beams with respect to the failure load under both load cases. It is clear from the figure that the beam section influences the failure load significantly. The failure load increases with an increase of the axial stiffness and flexural stiffness of beams. When the beam axial stiffness and flexural stiffness are reduced by 30% and 40% from the basic model, the failure loads decrease by 38 % and 40% for symmetrical and anti-symmetrical loads, respectively. When the beam axial stiffness and flexural stiffness are set twice those of the standard model, the failure loads increase by 69% and 83% for each load case, respectively. Therefore, the results show the beam section improves the stability performance of the hybrid barrel vault notably.

4.3 The influence of cables

The pre-stress and area of cables are also important factors that affect the elasto-plastic buckling behavior of the hybrid barrel vault. The failure load against the area of cables at the specified cable pre-stress of 100 MPa is shown in Fig. 14. The diameters of cables correspond to 8 mm, 10 mm, 12 mm, 15 mm and 20 mm in Fig. 13, respectively. It can be seen that the failure load increases with the rise of the cable area for the symmetrical load. However, the influence of

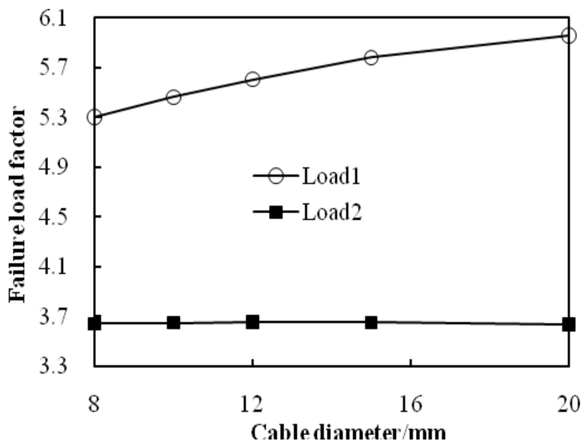

Fig. 14 Failure loads with different areas of cables

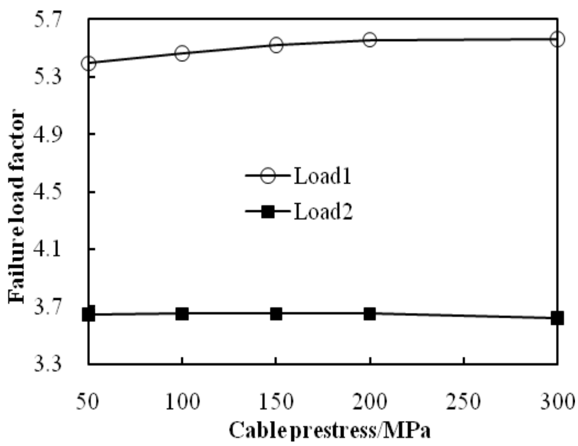

Fig. 15 Failure loads with different cable pre-stress

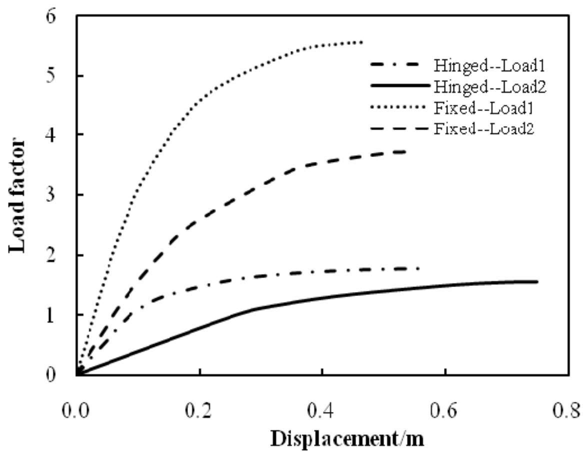

Fig. 16 Load–deflection curves of the hybrid structure with different support conditions

cable area on structural buckling capacity is not significant. Given the area of cables multiplied by 6.25 (where the diameter of cables increases from 8 mm to 20 mm), the failure load just increases by about 30%. When the structure is under the anti-symmetrical load, the failure load is almost not affected by the area of cables.

To study the effect of different pre-stress values directly, the initial stresses are set to 50 MPa, 100 MPa, 150 MPa, 200 MPa and 300 MPa, respectively. The failure load under both load cases versus the pre-stress of cables is shown in Fig. 15. It can be seen that the differences in failure loads are very small. For the pre-stresses considered in Fig. 15, the range of the variation of failure loads is within 1%.

Therefore, it is not an economical way to improve the stability capability of hybrid barrel vaults by increasing the pre-stress forces and areas of cables only.

4.4 The influence of boundary conditions

In all the cases mentioned above, the supports of hybrid barrel vaults are regarded as fixed. The elasto-plastic stability of hybrid barrel vaults with pinned supports is discussed in this section. The load-displacement curves with fixed and pinned supports under symmetrical and anti-symmetrical loads are shown in Fig. 16.

The figure indicates that there is a large difference of failure loads between fixed and pinned support vaults. Under the two support conditions, although the trend of these curves is similar, the failure load levels are quite different, as shown in Fig. 16. The failure load factor of the structure with pinned supports is 1.79 and 1.56 for the two load cases, respectively. Note the difference of the failure load with pinned supports between the two load cases is little. According to the results from the analysis, the maximum difference in the failure load between the two support conditions is up to 68% and 58% for both load cases. As a result, the effect of support conditions on the elasto-plastic stability should be taken into account in the design of the hybrid barrel vault.

5. Conclusions

The buckling capacity of the hybrid barrel vault was investigated in this paper. Eigenvalue buckling and geometrical non-linear elastic buckling analyses were carried our firstly. By taking into consideration of material non-linearity using elasto-plastic analyses, the behaviour of hybrid structures was found significantly different, which can only be revealed by large amount of geometrical and material non-linear simulations. Then the effects of different geometrical, structural, and load parameters on the failure loads were studied.

By comparing the results of analyses, conclusions can be drawn as follows:

- The effect of material non-linearity on the stability of the structure is significant; the buckling capacity is rapidly reduced taking account of material non-linearity. The plastic zone is firstly observed on both ends of the structure, and then gradually expands to the middle of the structure until failure.
- The stability of a hybrid barrel vault is sensitive to the anti-symmetrical distribution of load.
- The hybrid structure is highly imperfection sensitive and the reduction of the failure load due to imperfections can be considerable. Furthermore, when imposing imperfections, the proper shape and scale of the imperfection are important. The results show that the first eigenmode is the most critical imperfection shape.
- The analysis results show that under a particular span, the buckling capacity initially increases with the increase of the rise-to-span ratio and then decreases afterwards. Therefore, there exists an optimal rise-to-span ratio resulting in a relatively high buckling capacity for a specific span. Moreover, increasing the cross-section of steel beams notably improves the stability performance of the structure. However, the area and pre-stress of cables pose virtually no effect on the structural stability.
- The effect of the boundary conditions on the failure load is found notable.

Demand for glass roof system with longer span is increasing, and further research is required to improve the structural form in terms of static, dynamic, and stability capacity. The above conclusions are drawn from the work of this paper that has not considered the eccentricity and semi-rigidity of joints. Further investigations addressing these details are needed in future.

Acknowledgements

The work presented in this article was supported by the National Natural Science Foundation of China (Grant No. 51278116 and 51008065), Jiangsu "Six Top Talent" Program of China (Grant No.07-F-008), the Priority Academic Program Development of Jiangsu Higher Education Institutions and Scientific Research Foundation of Graduate School of Southeast University. The authors also deeply appreciate the remarks and suggestions of anonymous referees, which led to improvements in this paper.

References

Borri, C. and Spinelli, P. (1998), "Buckling and post-buckling behavior of single layer reticulated shells affected by random imperfections", *Comp*. *Struct*., **30**(4), 937-943.

Bulenda, T. and Knippers, J. (2001), "Stability of gird shells", *Comp*. *Struct*., **79**(12), 1161-1174.

Chen, X. and Shen, S.Z. (1993), "Complete load–deflection response and initial imperfection analysis of single-layer lattice dome", *Int. J. Space Struct.*, **8**(4), 271-278.
Eurocode 3 (2004), *European standard 3: Design of steel structures, Parts 1–6: Strength and Stability of Shell Structures*, European Committee for Standardization.
El-Sheikh, A. (2001a), "Configurations of single-Layer barrel vaults", *Adv. Struct. Eng.*, **4**(2), 53-64.
El-Sheikh, A. (2001b), "Performance of single-layer barrel vaults with different configurations", *Int. J. Space Struct.*, **16**(2), 111-123.
Fan, F., Wang, D.Z., Zhi, X.D. and Shen, S.Z. (2010a), "Failure modes of reticulated domes subjected to impact and the judgment", *Thin-Walled Struct.*, **48**: 143-149
Fan, F., Cao, Z.G. and Shen, S.Z. (2010b), "Elasto-plastic stability of single-layer reticulated shells", *Thin-Walled Struct.*, **48**(10-11), 827-836.
Forman, S.E. and Hutchinson, J.W. (1970), "Buckling of reticulated shell structures", *Int. J. Solids Struct.*, **6**(7), 909-932.
Gioncu, V. (1995), "Buckling of reticulated shells state-of-the-art", *Int. J. Space Struct.*, **10**(1), 1-46.
Gioncu, V. (2003), "Stability theory: Principles and methods for design of steel structures", *J. Constr. Steel Res.*, **59**(2), 269-270.
Gosowski, B. (2003), "Spatial stability of braced thin-walled members of steel structures", *J. Constr. Steel Res.*, **59**(7), 839-865.
Hosozawa, O., Shimamura, K. and Mizutani, T. (1999), "The role of cables in large span spatial structures: introduction of recent space structures with cables in Japan", *Eng. Struct.*, **21**, 795-804.
Kato, S., Yamashita, T. and Ueki, T. (2000), "Evaluation of elasto-plastic buckling strength of two-way grid shells using continuum analogy", In: *Sixth Asian Pacific Conference on Shell and Spatial Structures*, Seoul, Korea (International Association for Shell and Spatial Structures), 105-114.
Kang, W., Chen, Z., Lam, H.F. and Zuo, C. (2003), "Analysis and design of the general and outmost-ring stiffened suspen-dome structures", *Eng. Struct.*, **25**(13), 1685-1695.
Kitipornchai, S., Kang, W., Lam, H.F. and Albermani, F. (2005), "Factors affecting the design and construction of lamella suspen-dome systems", *J. Constr. Steel Res.*, **61**(6), 764-785.
Luo, Y.F. (1991), "Elasto-plastic stability and loading complete-process research of reticulated shells", Ph.D. Thesis, Tongji University. [in Chinese]
Meek, J.L. and Tan, H.S. (1984), "Geometrically non-linear analysis of space frames by an incremental iterative technique", *Comput. Methods Appl. Mech. Eng.*, 4**7**(3), 261-282.
Nee, K.M. and Halder, A. (1988), "Elasto-plastic non-linear post-buckling analysis of partially restrained space structure", *Comput. Methods Appl. Eng.*, **71**(1), 69-97.
Nie, G.H. (2003), "On the buckling of imperfect squarely-reticulated shallow spherical shells supported by elastic media", *Thin-Walled Struct.*, **41**(1), 1-13.
Saitoh, M. and Okada, A. (1999), "The role of string in hybrid string structures", *Eng. Struct.*, **21**(8), 756-769.
Schlaich, J. and Schober, H. (1996), "Glass-covered gird-shells", *Struct. Eng. Int.*, **6**(2), 88-90.
Suzuki, T., Ogawa, T. and Ikarashi, K. (1992), "Elasto-plastic buckling analysis of rigidly jointed single layer reticulated domes", *Int. J. Space Struct.*, **7**(4), 363-368.
JGJ61 (2003), *Technical Specification for Reticulated Shells*, Beijing, China Architecture Industry Press. [in Chinese]
Xue, W. and Liu, S. (2008), "Studies on a large-span beam string pipeline crossing", *J. Struct. Eng. ASCE*, **134**(10), 1657-1667.
Yamada, S., Takeuchi, A., Tada, Y. and Tsutsumi, K. (2001), "Imperfection-sensitive overall buckling of single-layer lattice domes", *J. Eng. Mech.*, **127**(4), 382-396.
Zhang, A.L. Zhang, X.F., Ge, J.Q. Liu, X.C. Wang, D.M. and Zhang, B.Q. (2006), "Influence of initial geometrical imperfections on stability of a suspendome for badminton arena for 2008 Olympic Games", *Spatial Struct.*, **12**(4), 8-12. [in Chinese]

CC